

Numerical Calculation of the Portal Pressure Gradient of the Human Liver With a Domain Decomposition Method

Zeng Lin, Bokai Wu, Shanlin Qin, Xinhong Wang, Rongliang Chen, and
Xiao-Chuan Cai

1 Introduction

Portal hypertension (PH) refers to the abnormal increase of the portal venous pressure, which is a common chronic liver disease with clinical consequences of cirrhosis, such as hepatic encephalopathy, variceal hemorrhage and ascites [11, 7]. Fig. 1 shows the portal vein and hepatic vein extracted from CT images, from the figure we also see the single inlet and multiple outlets structure of the portal vein and the multiple inlets and single outlet characteristics of the hepatic vein. The portal pressure gradient (PPG) is defined as the difference in the pressure between the inlet of the portal vein and the outlet of the inferior vena cava. PH refers to the situation that PPG is greater than 5 mmHg [4]. When the value of PPG is higher than 10 mmHg, the PH is

Zeng Lin

Shenzhen Institute of Advanced Technology, Chinese Academy of Sciences, Shenzhen, China,
e-mail: zeng.lin@siat.ac.cn

Bokai Wu

Shenzhen Institute of Advanced Technology, Chinese Academy of Sciences, Shenzhen, China,
e-mail: bk.wu@siat.ac.cn

Shanlin Qin

Shenzhen Institute of Advanced Technology, Chinese Academy of Sciences, Shenzhen, China,
e-mail: sl.qin@siat.ac.cn

Xinhong Wang

Department of Radiology, The Second Affiliated Hospital, School of Medicine, Zhejiang University,
Hangzhou, China, e-mail: 2611104@zju.edu.cn

Rongliang Chen

Shenzhen Institute of Advanced Technology, Chinese Academy of Sciences, Shenzhen, China,
e-mail: rl.chen@siat.ac.cn

*Corresponding Author: Xiao-Chuan Cai

Department of Mathematics, University of Macau, Macau, China, e-mail: xccai@um.edu.mo

called the clinically significant portal hypertension. If PPG is higher than 12 mmHg, variceal hemorrhage may occur [11].

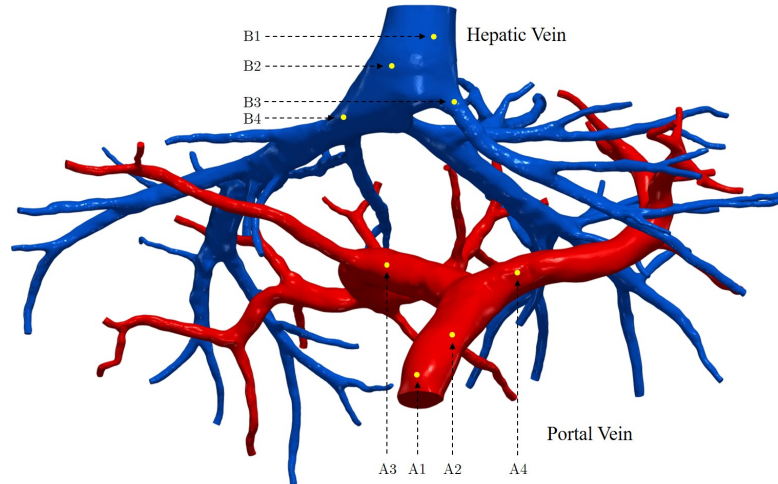


Fig. 1: The segmented portal vein and hepatic vein

In clinical applications, the common approach to measure the PPG is the trans-jugular route, which requires the insertion of a radiopaque catheter into the right hepatic vein via the jugular vein under fluoro scopic guidance. The method is invasive and sometimes impractical for routine clinical practice. Recently, a technology based on computational fluid dynamics (CFD) [5, 6, 14] is being introduced as an alternative approach to measure the pressure difference non-invasively. With CFD, several desired pathological values, such as pressure, velocity and wall shear stress (WSS) can be easily computed.

In this work, we model the blood flow by the system of Navier-Stokes equations which is discretized by a fully implicit finite element method on a fully unstructured mesh, and solved by an efficient and highly parallel domain decomposition method [9]. With this method, a simulation of a full 3D patient-specific hepatic flow can be realized in a few hours. The numerical experiments are carried out on a cluster of computers with near 2000 processor cores and the parallel efficiency is higher than 60%. The computed PPG values are within the normal range of published data.

2 Numerical method

The blood flows in the hepatic vessels are described by the unsteady incompressible Navier-Stokes equations:

$$\begin{cases} \rho \frac{\partial \mathbf{u}}{\partial t} + \rho(\mathbf{u} \cdot \nabla)\mathbf{u} - \nabla \cdot \boldsymbol{\sigma} = \mathbf{f} & \text{in } \Omega \times (0, T], \\ \nabla \cdot \mathbf{u} = 0 & \text{in } \Omega \times (0, T]. \end{cases} \quad (1)$$

Here \mathbf{u} denotes the velocity vector, ρ the blood density, \mathbf{f} the external force and $\boldsymbol{\sigma}$ is the Cauchy stress tensor defined as:

$$\boldsymbol{\sigma} = -p\mathbf{I} + 2\mu\boldsymbol{\varepsilon}(\mathbf{u}), \quad (2)$$

where p is the pressure, \mathbf{I} is the identity tensor, μ is the dynamic viscosity and $\boldsymbol{\varepsilon}$ is the deformation tensor defined as $\boldsymbol{\varepsilon}(\mathbf{u}) = 1/2(\nabla\mathbf{u} + \nabla\mathbf{u}^T)$.

The initial condition is imposed by a given function. The velocity boundary conditions are imposed for the inlets of the portal vein. No slip condition is applied on the wall. The resistance boundary conditions are used for the outlets of the portal vein and hepatic vein [8].

The weak form of (1) reads: Find $\mathbf{u} \in V$ and $p \in P$ such that $\forall \mathbf{v} \in V_0$ and $\forall q \in P$,

$$\mathbf{B}(\{\mathbf{u}, p\}, \{\mathbf{v}, q\}) = 0, \quad (3)$$

where

$$\begin{aligned} \mathbf{B}(\{\mathbf{u}, p\}, \{\mathbf{v}, q\}) = & \rho \int_{\Omega} \frac{\partial \mathbf{u}}{\partial t} \cdot \mathbf{v} d\Omega + \rho \int_{\Omega} (\mathbf{u} \cdot \nabla)\mathbf{u} \cdot \mathbf{v} d\Omega \\ & - \int_{\Omega} p(\nabla \cdot \mathbf{v}) d\Omega + 2\mu \int_{\Omega} \boldsymbol{\varepsilon}(\mathbf{u}) : \boldsymbol{\varepsilon}(\mathbf{v}) d\Omega \\ & + \int_{\Omega} (\nabla \cdot \mathbf{u})q d\Omega + \int_{\Gamma_O} (\boldsymbol{\sigma}\mathbf{n}) \cdot \mathbf{v} d\Gamma - \rho \int_{\Omega} \mathbf{f} \cdot \mathbf{v} d\Omega. \end{aligned} \quad (4)$$

Here Γ_O is the outlet boundary and \mathbf{n} is the outward normal vector of the outlet. The functional spaces V , V_0 and P are defined in details in [5].

The computational domain Ω is covered with a fully unstructured tetrahedral mesh on which we introduce $P_1 - P_1$ finite element function spaces. As the $P_1 - P_1$ pair doesn't satisfy the Ladyzhenskaya-Babuska-Brezzi (LBB) [2] condition, some stabilization terms are added in the weak form (4) when applied to finite element functions. More details about the stabilization parameters can be found in [2]. Then (4) can be rewritten as a time-dependent nonlinear algebraic system

$$\frac{d\mathbf{X}(t)}{dt} = \mathcal{N}(\mathbf{X}), \quad (5)$$

where $\mathbf{X}(t)$ is the vector of the nodal values of the velocity \mathbf{u} and pressure p , $\mathcal{N}(\cdot)$ is the nonlinear function representing the spatial discretization of (4). (5) can be further discretized by the fully implicit backward Euler method in time

$$\frac{\mathbf{X}^n - \mathbf{X}^{n-1}}{\Delta t} = \mathcal{N}(\mathbf{X}^n), \quad (6)$$

where \mathbf{X}^n is the value of $\mathbf{X}(t)$ at the n -th time step and Δt is the time step size.

For simplicity, (6) can be rearranged into a nonlinear system

$$\mathcal{F}^n(\mathbf{X}^n) = 0 \quad (7)$$

to be solved at each time step.

In this work, the nonlinear system (7) will be solved by the Newton-Krylov-Schwarz algorithm [13]. The algorithm includes three components, an inexact Newton [3] as the nonlinear solver, a preconditioned Krylov subspace method (GMRES) [12] as the linear solver at each Newton step, and an overlapping Schwarz method [1] as the preconditioner. More details about the algorithm are available in [8].

3 Numerical experiments

In this section, we present some numerical experiments for blood flows in the portal vein and hepatic vein, and also the parallel performance of the algorithm with respect to the number of processor cores. Lastly, the PPG values will be calculated based on the simulation of blood flows in a patient-specific portal vein and hepatic vein.

In all the numerical experiments, $\rho = 1.05g/cm^3$ and $\mu = 0.038cm^2/s$ [10] are used to characterize the properties of the hepatic blood. The algorithm is implemented with the Portable Extensible Toolkit for Scientific computation (PETSc) library. In the experiments, the relative stopping condition for Newton is set to be 1.0×10^{-6} and the relative stopping condition for GMRES is 1.0×10^{-3} . Incomplete LU (ILU) is used to solve the subdomain problems in the additive Schwarz preconditioner. “ILU(l)” represents ILU with l level of fill-ins, “ np ” means the number of processor cores, “Newton” stands for the average number of Newton iterations per time step, “GMRES” denotes the average number of GMRES iterations per Newton step, “Time” is the average wall clock time in seconds spent per time step, “Memory” indicates the memory consumption in megabyte per processor core per time step, “Speedup” denotes the speedup ratio and “Efficiency” means the parallel efficiency.

A sample finite element mesh for the portal vein and hepatic vein is shown in Fig. 2. The portal vein has 1 inlet and 25 outlets and the hepatic vein has 47 inlets and 1 outlet. The clinically measured flow velocity [10] is used for the inflow boundary condition and the total resistance is chosen such that the computed pressures are within the ranges of typical adult patients.

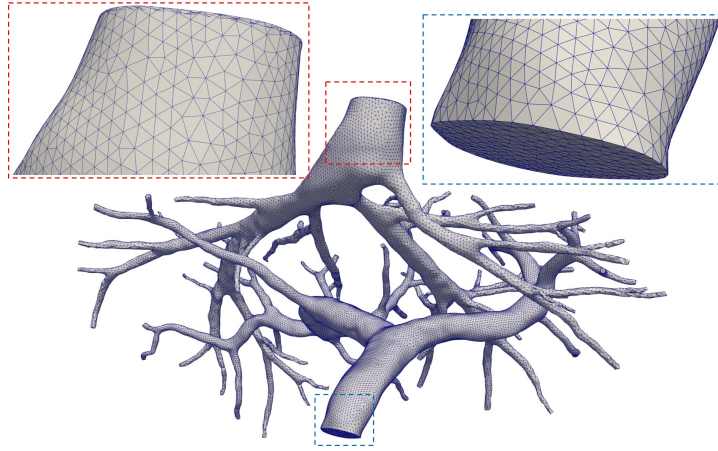


Fig. 2: A sample finite element mesh for the portal vein and hepatic vein

Table 1: Parallel performance using different number of processor cores

np	Newton	GMRES	Memory (MB)	Time (s)	Speedup	Efficiency
240	3.10	404.52	450.89	160.39	1	100%
480	3.10	452.68	250.55	93.97	1.71	86%
960	3.10	457.98	143.06	51.93	3.09	77%
1920	3.10	462.02	78.84	30.14	5.32	67%

A parallel scalability study. The parallel scalability is investigated on a cluster of computers, and each compute node of the computer has two Intel Xeon processors and 64GB of shared memory. The performance of the algorithm in terms of the number of Newton iterations per time step, the number of GMRES iterations per Newton step, the total memory per processor core per time step, the total compute time per time step, the speedup ratio and the parallel efficiency are presented in Table 1. A mesh with 9.96×10^6 elements is utilized for the numerical tests, where the largest size of the elements is $0.85mm$, the smallest is $0.09mm$ and the average is $0.26mm$. The time step size is set as $\Delta t = 1.00 \times 10^{-3}s$, the subdomain solver is ILU(1) and the overlapping size is 2. The scalability about the linear and nonlinear algebraic solvers are clearly observed, wherein the number of Newton iterations and GMRES iterations change only slightly as the number of processor cores increase, especially for the Newton iterations. It can be seen that when the number of processor cores increases from 240 to 1920, the compute time reduces to $30.14s$ and the parallel efficiency reduces to 67%, which is quite good considering the fact that the geometry of the problem is rather complicated.

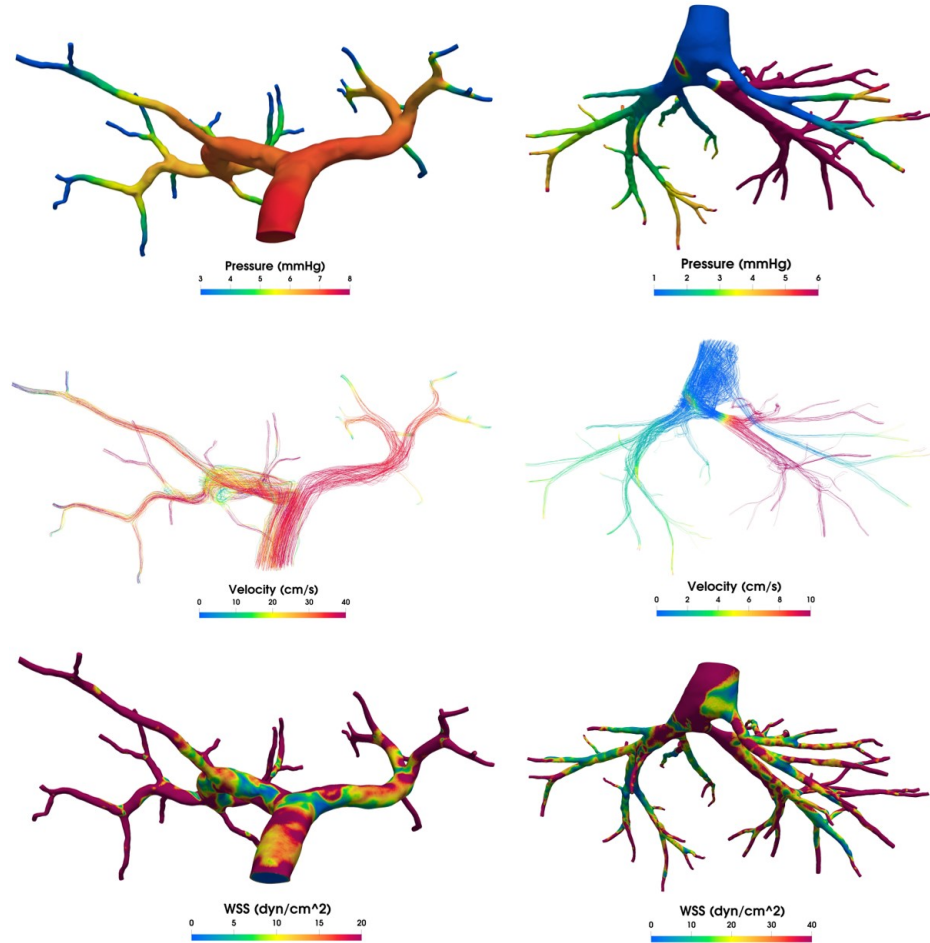


Fig. 3: The pressure, velocity and WSS distribution of the computed flow in the portal vein and hepatic vein at $t = 0.5s$

The portal pressure gradient. Next, we present a numerical calculation of PPG. Firstly, the pressure, velocity and WSS distributions of the blood flow in the portal vein and hepatic vein at $t = 0.5s$ are plotted in Fig. 3. Then we pick several pairs of points (A1,B1), (A2,B2), (A3,B3) and (A4,B4) as marked in Fig. 1 to compute the difference in the pressure between the portal vein and the hepatic vein, i.e., the PPG, for three cardiac cycles. The portal vein pressure at points A1, A2, A3 and A4 are drawn in the top-left sub-figure of Fig. 4. Meanwhile, the hepatic vein pressure at points B1, B2, B3 and B4 are illustrated in the top-right sub-figure of Fig. 4. Then their PPG values of the pairs (A1,B1), (A2,B2), (A3,B3) and (A4,B4) are plotted in the bottom-left sub-figure of Fig. 4. Finally, the time-averaged PPG (TAPPG)

values are presented in the bottom-right sub-figure of Fig. 4. It is clear that all four approximations are within the normal ranges as indicated in [8].

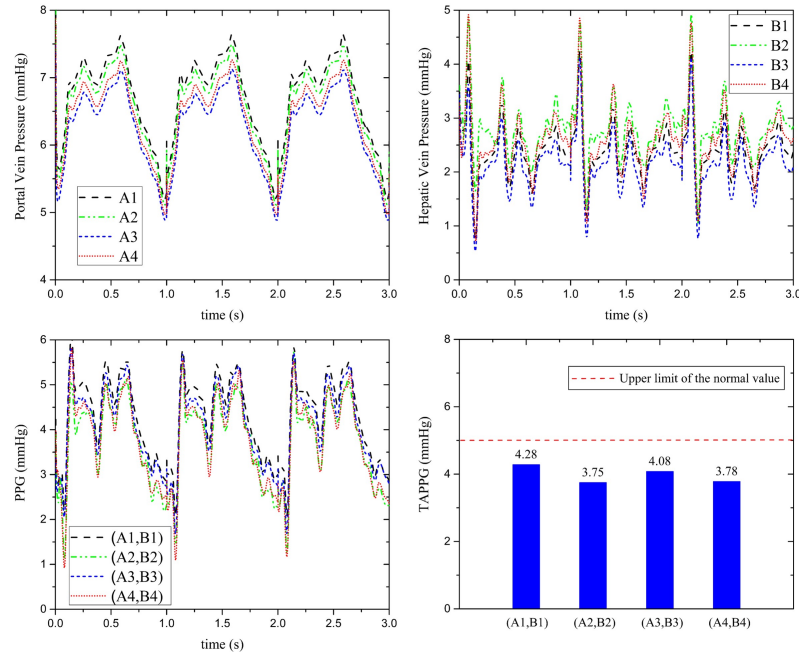


Fig. 4: The computed portal vein pressure, hepatic vein pressure, PPG and TAPPG values for three cardiac cycles

References

1. Xiaochuan Cai and Marcus Sarkis. A restricted additive schwarz preconditioner for general sparse linear systems. *SIAM Journal on Scientific Computing*, 21(2):792–797, 1999.
2. Rongliang Chen, Yuqi Wu, Zhengzheng Yan, Yubo Zhao, and Xiao-Chuan Cai. A parallel domain decomposition method for 3d unsteady incompressible flows at high reynolds number. *Journal of Scientific Computing*, 58(2):275–289, 2014.
3. Stanley C Eisenstat and Homer F Walker. Choosing the forcing terms in an inexact newton method. *SIAM Journal on Scientific Computing*, 17(1):16–32, 1996.
4. Jason Y Huang, Jason B Samarasena, Takeshi Tsujino, John Lee, Ke-Qin Hu, Christine E McLaren, Wen-Pin Chen, and Kenneth J Chang. Eus-guided portal pressure gradient measurement with a simple novel device: a human pilot study. *Gastrointestinal endoscopy*, 85(5):996–1001, 2017.
5. Fande Kong, Vitaly Kheyfets, Ender Finol, and Xiao-Chuan Cai. An efficient parallel simulation of unsteady blood flows in patient-specific pulmonary artery. *International journal for numerical methods in biomedical engineering*, 34(4):e2952, 2018.

6. Fande Kong, Vitaly Kheyfets, Ender Finol, and Xiao-Chuan Cai. Simulation of unsteady blood flows in a patient-specific compliant pulmonary artery with a highly parallel monolithically coupled fluid-structure interaction algorithm. *International Journal for Numerical Methods in Biomedical Engineering*, 35(7):e3208, 2019.
7. Jia-Yun Lin, Chi-Hao Zhang, Lei Zheng, Hong-Jie Li, Yi-Ming Zhu, Xiao Fan, Feng Li, Yan Xia, Ming-Zhe Huang, Sun-Hu Yang, et al. Establishment and assessment of the hepatic venous pressure gradient using biofluid mechanics (hvpgbfm): protocol for a prospective, randomised, non-controlled, multicentre study. *BMJ open*, 9(12):e028518, 2019.
8. Zeng Lin, Rongliang Chen, Beibei Gao, Shanlin Qin, Bokai Wu, Jia Liu, and Xiao-Chuan Cai. A highly parallel simulation of patient-specific hepatic flows. *International Journal for Numerical Methods in Biomedical Engineering*, page e3451, 2021.
9. Li Luo, Wen-Shin Shiu, Rongliang Chen, and Xiao-Chuan Cai. A nonlinear elimination preconditioned inexact newton method for blood flow problems in human artery with stenosis. *Journal of Computational Physics*, 399:108926, 2019.
10. Renfei Ma, Peter Hunter, Will Cousins, Harvey Ho, Adam Bartlett, and Soroush Safaei. Anatomically based simulation of hepatic perfusion in the human liver. *International journal for numerical methods in biomedical engineering*, 35(9):e3229, 2019.
11. Xiaolong Qi, Weimin An, Fuquan Liu, Ruizhao Qi, Lei Wang, Yanna Liu, Chuan Liu, Yi Xiang, Jialiang Hui, Zhao Liu, et al. Virtual hepatic venous pressure gradient with ct angiography (chess 1601): a prospective multicenter study for the noninvasive diagnosis of portal hypertension. *Radiology*, 290(2):370–377, 2019.
12. Youcef Saad and Martin H Schultz. Gmres: a generalized minimal residual algorithm for solving nonsymmetric linear systems. *Siam Journal on Scientific and Statistical Computing*, 7(3):856–869, 1986.
13. Yuqi Wu and Xiao-Chuan Cai. A parallel two-level method for simulating blood flows in branching arteries with the resistive boundary condition. *Computers & fluids*, 45(1):92–102, 2011.
14. Nan Xiao, Jay D Humphrey, and Figueroa C. Alberto. Multi-scale computational model of three-dimensional hemodynamics within a deformable full-body arterial network. *Journal of Computational Physics*, 244:22–40, 2013.